Chapter 79
Frequency- and Distance-Dependent Relation Between Event-Related EEG Activity and BOLD Responses in an Auditory Stroop Paradigm

T.A. Kranz, N. Axmacher, P. Trautner, K. Lehnertz and J. Fell

Abstract The exact relationship between electroencephalogram (EEG) and blood oxygenation level-dependent (BOLD) responses in functional magnetic resonance imaging (fMRI) recordings is still an open question, in particular for event-related cognitive paradigms. Here, we investigated how the relationship between event-related power changes in the EEG (ERPC) and BOLD responses varies for the typical EEG frequency bands and depending on the distance between the fMRI voxel and the EEG recording site. As cognitive task we chose an auditory Stroop experiment. We observed that for small distances event-related BOLD responses were positively correlated with ERPC in the gamma band, just as, in contrast to previous studies, in the alpha band. BOLD responses were negatively correlated with EEG power in the delta range for regions close to the EEG recording site.

Keywords EEG · FMRI · Simultaneous · Event-related · Interrelation · Stroop

T.A. Kranz · N. Axmacher · K. Lehnertz · J. Fell (✉)
Department of Epileptology, University of Bonn, Sigmund-Freud-Strasse 25, 53127 Bonn, Germany
e-mail: Juergen.Fell@ukb.uni-bonn.de

T.A. Kranz · K. Lehnertz
Helmholtz-Institute for Radiation and Nuclear Physics, University of Bonn, Nussallee 14-16, 53115 Bonn, Germany

K. Lehnertz
Interdisciplinary Center for Complex Systems, University of Bonn, Bruehlerstrasse 7, 53119 Bonn, Germany

P. Trautner
Department of NeuroCognition, Life and Brain Center Bonn, Sigmund-Freud-Str. 25, 53127 Bonn, Germany

R. Wang and X. Pan (eds.), *Advances in Cognitive Neurodynamics (V)*,
Advances in Cognitive Neurodynamics, DOI 10.1007/978-981-10-0207-6_79

79.1 Introduction

Electroencephalogram (EEG) and functional magnetic resonance imaging (fMRI) are well-established methods in the cognitive neurosciences. Both aim at measuring correlates of neural activity, but they exhibit substantial differences. While EEG is being used to directly measure electrical brain activity with a high temporal resolution, fMRI monitors the blood oxygenation level-dependent (BOLD) response, which is caused by metabolic processes and has a low temporal resolution, but excels noninvasive EEG in its superior spatial resolution and its ability to investigate deep brain structures.

The strongly orthogonal characteristics of EEG and fMRI brought up the idea of multimodal measurements, combining the advantages of both approaches. Early studies identified the difficulties of this endeavor, for instance [1, 2]. The main challenge is to guarantee a sufficient quality of the EEG signal, as it is contaminated by various kinds of artifacts generated by the magnetic fields involved in magnetic resonance imaging (MRI). Numerous approaches were implemented. Initial attempts used epileptic potentials on the EEG from epilepsy patients to trigger acquisition of single fMRI volumes [1, 2]. With new techniques such as average artifact subtraction or principal component analysis [3–6] (quasi) simultaneous measurements became possible, thus laying the foundation for new applications of the combined EEG/fMRI approach, including search for generators of the alpha rhythm [7–9], event-related studies with visual/auditory stimuli [10–12], and analyses of sleep-stage dependent brain activity [13, 14].

Notwithstanding the progress achieved in the field of simultaneous EEG and fMRI [15], many questions remain. Previous studies, e.g., [7, 10, 13, 16, 17], indicate that the EEG–BOLD relation for ongoing (spontaneous) and event-related (task-induced) EEG oscillations appear to be different. For example, while spontaneous alpha (8–12 Hz) activity appears to be clearly related to a reduction of BOLD responses [7], results for task-induced alpha are less clear, e.g., depending on the brain region the correlation might be positive [18] or this correlation might be linked to the overall brain activity in a broader frequency range [19].

Furthermore, it is still an open question how localized the BOLD responses corresponding to EEG signal changes are: BOLD responses related to EEG oscillations may be generated within very restricted brain regions or within larger areas. The relatively high spatial resolution of fMRI as compared to EEG allows to address this question. In fact, the abundant occurrence of center-surround inhibition in the brain—i.e., the fact that local activations are often related to adjacent inhibitions—may even suggest that local positive EEG–BOLD correlations are accompanied by surrounding negative correlations.

Finally, the relationship between BOLD responses and EEG oscillations may differ for fast as compared to slow oscillations. In general, slow oscillations appear to be generated by wide-spread neural networks, while faster oscillations seem to be due to more localized mechanisms (e.g., [20]). Moreover, slow oscillations were

often found to be related to cortical deactivation, whereas fast oscillations are often associated with cortical activation (e.g., [21]).

Here, we aimed at investigating how the relationship of EEG oscillations and BOLD responses varies with EEG frequency and the distance between the fMRI voxel and the EEG recording site. Event-related EEG oscillations were induced by a Stroop experiment involving cognitive processing related to conflicts. We implemented an interleaved design of quasi-simultaneous EEG/fMRI recordings, i.e., all stimulus presentations were scheduled during repetitive pauses between the acquisitions of fMRI volumes in order to keep the influence of noise on event-related EEG activity as low as possible. Additionally, to reduce artifacts caused by head and eye movements, we used an auditory version of the Stroop paradigm.

79.2 Materials and Methods

79.2.1 Subjects

Fourteen healthy subjects (ages 18–51, 32.5 ± 9.9 years, nine males) participated in the study. Eleven subjects were right-handed, only one was left-handed, and two were ambidexters according to the Edinburgh handedness inventory. The protocol was approved by the local Ethics committee and all subjects gave written informed consent.

79.2.2 Experimental Design

An auditory implementation of the established Stroop task [22] was presented to the subjects. During the experiment subjects closed their eyes. Three different words were presented (“high,” “low,” “good”), either in a high or a low tone pitch. The subjects were asked to decide whether the word was presented in a high or low tone pitch, regardless of the word meaning, and had to indicate the tone pitch by button press (left index finger: high, right index finger: low) within 2500 ms after stimulus presentation.

The stimuli could be grouped into three different experimental conditions: when one of the words “high” or “low” was presented, the tone pitch could be *congruent* or *incongruent* while presentations of the word “good” formed a *control* condition (actually, the German words “hoch,” “tief,” and “gut” were used). The *incongruent* condition implies a processing conflict. In contrast, carrying out the alternative task, i.e., semantic processing of the word, is a more automatic cognitive process and thus less conflict-prone.

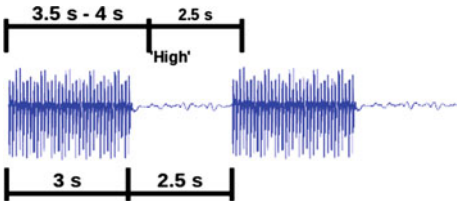

Fig. 79.1 Experimental design. The experiment consisted of 120 trials (40 x "high," "low," "good," each 50 % low tone pitch). Presentation of the stimuli was synchronized with the fMRI volume acquisition. In every second intermission a stimulus was presented. The sounds were presented for 500 ms. Subjects had to indicate the tone pitch by button press within 2500 ms after stimulus presentation. Trials were separated by an inter-trial interval of 10.75–11.25 s

We used the same auditory stimuli as [23]. Recording and digital postprocessing were accomplished using the Goldwave audio editing software [24]. In order to transpose the stimuli to high or low tone pitch the Entropic Timescale Modification (ETSM^{TM}) was applied.

We used Presentation Version 13 (Neurobehavioural Systems, Albany, CA, USA) for the implementation of the paradigm. The presentation of the stimuli was interleaved with the fMRI volume acquisition in order to keep the event-related potentials unaffected by gradient artifacts (see Fig. 79.1). Furthermore, the presentation of the auditory stimuli was thus less superposed by the humming scanner noise. We used a jitter of ±250 ms to prevent the stimulus presentation from being time-locked to the imaging artifacts.

79.2.3 EEG Aquisition

EEG activity was recorded from 29 scalp positions using sintered silver–chloride electrodes mounted on a cap system (Diamedic, Munich, Germany). The signals were preamplified within the MRI scanner and then transformed into optical signals. We used a DC-powered Brainlab EMR 32 amplifier (Schwarzer, Munich, Germany) specifically designed for the use in simultaneous EEG/fMRI experiments. The amplified data were digitized at a sampling rate of 1000 Hz within a bandwidth of 0.02–200 Hz. Arrangements were taken to keep the electrode–skin impedances below 5 kΩ during measurements, and impedances were checked before and after the measurement.

79.2.4 Preprocessing of EEG Data

To achieve a satisfying quality of the EEG signal, we applied custom filter routines in order to reduce the gradient and pulse artifacts (see Fig. 79.2). In the first step we

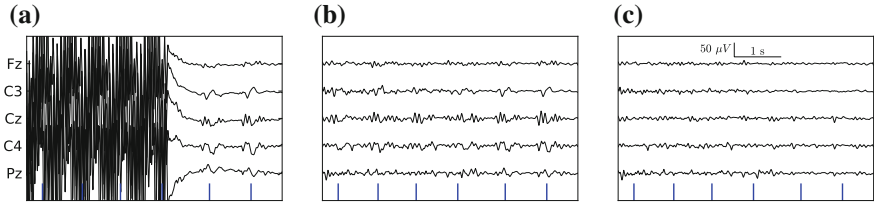

Fig. 79.2 Exemplary depiction of the filter process. **a** Unfiltered EEG segment corresponding to one fMRI volume acquisitions (TR = 5.5 s). **b** In a first step, the high-amplitude gradient artifacts were reduced, the BCG artifacts dominate the EEG traces (BCG artifacts are marked with *blue lines*). **c** Then the BCG waveforms were identified and removed (Color figure online)

reduced the gradient artifacts by a combination of average artifact subtraction (cp. [5]) and principal component analysis techniques. For ballistocardiogram (BCG) artifact reduction we modified this method in two aspects. First, we implemented a reliable semi-automatic approach for determining the timepoints when BCG artifacts occured. Second, all other occurrences of BCG artifacts were automatically identified by searching for timepoints with similar EEG patterns.

79.2.5 MRI Acquisition and Preprocessing

Structural and functional MRI data were collected at the Life & Brain Center, Bonn, using a 1.5 T AVANTO scanner (Siemens, Erlangen, Germany) and a total imaging matrix (TIM) head coil.

Functional data were acquired using a T_2^*-weighted slice-interleaved gradient-echo EPI sequence with 35 slices parallel to the line between the anterior and the posterior commissure and a 64 × 64 matrix. The TR was 5.5 s consisting of a volume acquisition time of 3 s and a intermission of approximately 2.5 s in every cycle. Further parameters were $T_E = 5\,\text{ms}$, voxel-size $3\,\text{mm} \times 3\,\text{mm} \times 3\,\text{mm}$, flip angle 90°, and field-of-view 192 mm.

For anatomical data, a T_1-weighted MPRAGE sequence (matrix size 256 × 256, field of view: 256 mm, 120 sagittal slices, slice thickness: 1 mm, inter-slice gap: 0.5 mm) was used. The field-of-view included the head surface and the EEG electrodes. These images were used to precisely determine the positions of the electrodes.

Functional data preprocessing was carried out using FMRI Expert Analysis Tool (FEAT) Version 5.98, part of FSL (FMRIB's Software Library, [25]). The 4d data were motion corrected, slice-timing corrected using Fourier-space time series phase-shifting, then non-brain parts were removed, and afterward the data were spatially smoothed using a Gaussian kernel with 5 mm FWHM. Finally, the 4d data were grand-mean intensity normalized using a single multiplicative factor and high-pass temporally filtered by a Gaussian-weighted least-squares straight line fitting with $\sigma = 50.0\,\text{s}$.

79.2.6 Combined Analysis of EEG and FMRI

The aim of our study was to examine whether the ERPC–BOLD relation varies with the EEG frequency band and the distance between EEG recording site and fMRI voxel. In brief, we chose the following approach (for details, please see below):

1. For each stimulus presentation we calculated ERPC in the $\delta, \theta, \alpha, \beta, \gamma_1, \gamma_2$ bands.
2. For each stimulus presentation and each voxel we estimated the amplitude of the BOLD signal for the timepoint that corresponds to the expected maximum of the hemodynamic response function (HRF).
3. For each EEG recording site, we defined multiple spatial *regions-of-interest* (ROIs) as those parts of the brain contained in spherical shells with different radii around the recording site. For each ROI we calculated the average BOLD amplitude over all voxels.
4. We calculated the correlation coefficients between ERPC (step 1) and average BOLD amplitude (step 3) for each frequency and each ROI.

In the following, these analysis steps are described in further detail:

Ad 1 For each recording site and each stimulus presentation, EEG time series from −1 to +2 s relative to stimulus onset were extracted, demeaned, and tapered by multiplying quarter sine waves to the first/last eighth of the data. We then band-pass filtered these time series by applying second-order Butterworth filters forward and backward in time and calculated the instantaneous power using the Hilbert transform. We chose the filter edge frequencies as follows: $\delta : [0.5, 3\ \text{Hz}]$, $\theta : [3, 7.5\ \text{Hz}]$, $\alpha : [7.5, 12\ \text{Hz}]$, $\beta : [12, 30\ \text{Hz}]$, $\gamma_1 : [30, 60\ \text{Hz}]$,[1] $\gamma_2 : [60, 80\ \text{Hz}]$. For each of these frequency bands, we calculated the temporally averaged ERPC within the interval $[0; 1000\ \text{ms}]$ by the mean pre-stimulus power obtained from the interval $[-200; 0\ \text{ms}]$.

Ad 2 For each voxel, we interpolated between the samples of the BOLD signal using cubic b-splines. For each stimulus presentation, we evaluated the splines at the timepoints of the expected maximum of the HRF as an estimate for the corresponding BOLD amplitude $A_{i,j}, i \in [1, N_\text{v}], j \in [1, N_\text{sp}]$ (N_v: number of voxels, N_sp: number of stimulus presentations). A priori we chose an offset of six seconds post stimulus according to the results of previous studies (e.g., [26]).

Ad 3 Around each EEG recording site we defined seven ROIs as spherical shells with the inner/outer radii 0, 20, 30, 40, 50, 60, 70, and 100 mm, i.e., the first (second) shell had an inner radius of 0 mm (20 mm) and an outer radius of 20 mm (30 mm), from now on denoted as, e.g., $R^{\text{I,O}} = 20, 30\ \text{mm}$. To do so, we first determined the EEG recording site locations using our program *PyLocator* (available at http://www.nipy.org). Here, we rendered a virtual representation of the head surface from structural MRI data of the subject using the *marching cubes algorithm*

[1] As the amplifier was DC-powered, line noise was not observed in the EEG signal.

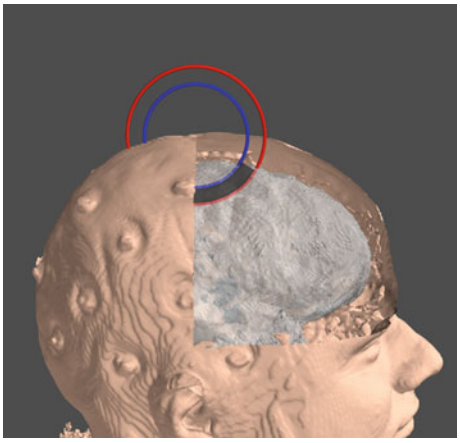

Fig. 79.3 Schematic representation of ROI definition. We located the EEG recording sites on a 3d reconstruction of the subject's head and then defined spherical shells with different radii (R^{I} *blue circle*, R^{O} *red circle*). Only those parts of the brain (estimated by BET [28], rendered in *light gray*) that were contained in these shells were included in the ROI (*dark gray*) (Color figure online)

as implemented in the *Visualization Toolkit* (VTK, [27]). In this representation, the electrodes, or more precisely the electrode gel, were visible as small distortions of the head surface. The locations of these distortions were marked and the corresponding coordinates were extracted. For each EEG recording site, we calculated its spatial distances to each voxel's center. If this distance was in the interval $[R^{\mathrm{I}}, R^{\mathrm{O}}]$, the voxel was regarded as part of the ROI (cp. Fig. 79.3). Only brain voxels were included in the analysis. We used BET ([28], part of FSL) to estimate the extent of brain tissue. For each $\mathrm{ROI}(R^{\mathrm{I}}, R^{\mathrm{O}}, k),\ k \in [1, N_e]$ (N_{s}: number of EEG recording sites) we calculated an average BOLD amplitude[2] $\bar{A}(R^{\mathrm{I}}, R^{\mathrm{O}}, j, k) = \frac{1}{|\mathrm{ROI}|} \sum_{i \in \mathrm{ROI}} A_{ij}, j \in [1, N_{\mathrm{sp}}], k \in [1, N_e]$.

Ad 4 For each combination of EEG recording site, frequency band, and ROI, we calculated Spearman's rank correlation coefficients ρ between the ERPC (step 1) and the corresponding average BOLD amplitude (step 3).

Due to signal quality considerations (BCG artifacts are more pronounced at lateral EEG recording sites) we performed the aforementioned steps of analysis only for the channels Fz, C3, Cz, C4, and Pz. We performed this entire procedure for stimulus presentations from the three conditions (*incongruent*, *congruent*, *control*) and for the union of these sets of trials (meta-condition *all*).

[2]For reasons of clearness we here use **ROI** as simplification for $\mathrm{ROI}(R^{\mathrm{I}}, R^{\mathrm{O}}, k)$.

79.3 Results

We first show behavioral results and event-related potentials (ERPs) as indicators (i) for the sanity of the Stroop task and its presentation and (ii) for the quality of the EEG recording and filtering. We do not discuss these results in detail (see e.g., [23, 29, 30]) as we focus on our findings addressing the interrelation between EEG band power and BOLD responses. These are presented afterwards.

79.3.1 Behavioral Data

The behavioral data for the three experimental conditions *congruent*, *incongruent* and *control* are shown in Fig. 79.4. Due to the conflict, accuracy during *incongruent* trials was lower than during *congruent* trials ($t = 5.75$, $p < 0.001$, Student's paired t-tests) and reaction times were longer ($t = -5.01$, $p < 0.001$). The results for the condition *control* were just between these two extremes but without any significant difference to any of these. In this case, the semantic meaning of the stimulus is neither in conflict nor in accordance to its phonetic properties, and thus neither supports nor interferes with successful task completion.

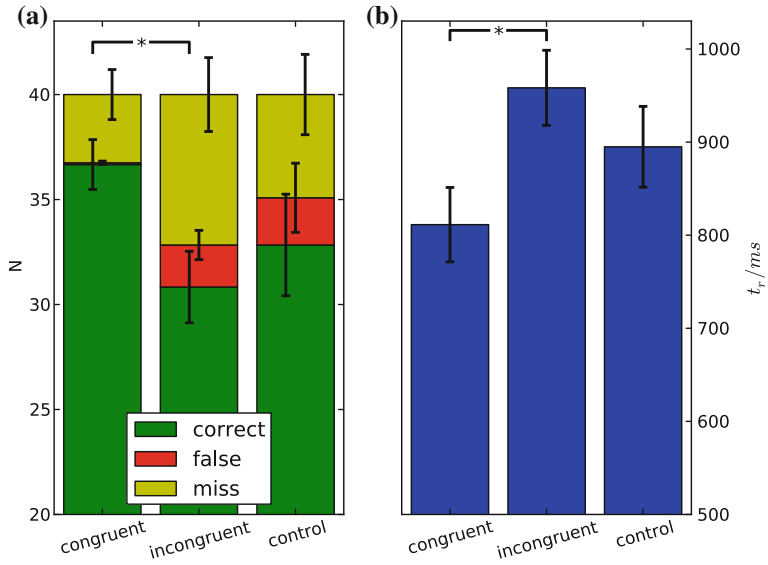

Fig. 79.4 Behavioral data. **a** Number of correct/false/missed responses for the three experimental conditions, averaged over 14 subjects. The number of correct responses was larger for condition *congruent* than for *incongruent* ($p < 0.001$). **b** Average reaction times (t_r) across subjects and all trials where a response was given. For *congruent* the reaction times were shorter than for *incongruent* ($p < 0.001$)

In accordance with previous studies (e.g., [31, 23]), our data show that the auditory Stroop task features similar conflict effects as the original visual Stroop task [32, 22].

79.3.2 Event-Related Potentials

Besides visual inspection of the preprocessed EEG, the event-related potentials served as a quality measure for our EEG recording and filtering process. Two subjects had to be excluded due to inferior quality of the recording resulting in insufficient filtering results. In three further subjects, there was a strong artifact induced in the EEG by the headphone. This was discovered only after all experimental sessions were completed and was limited to the presentation of the word "high." These trials were excluded from the analysis.

Figure 79.5 shows the event-related potentials for the three experimental conditions at electrodes Fz, C3, Cz, C4, and Pz. They feature a prominent N200 component. Additionally, more negative ERPs for the *incongruent* compared to the *congruent* condition between 300 and 500 ms poststimulus can be observed, very similar to the findings of [30] for a visual Stroop paradigm. ERP differences between experimental conditions were not analyzed further because the evaluation of the EEG–BOLD interrelation (see below) revealed no effect for or interaction with the factor *condition*.

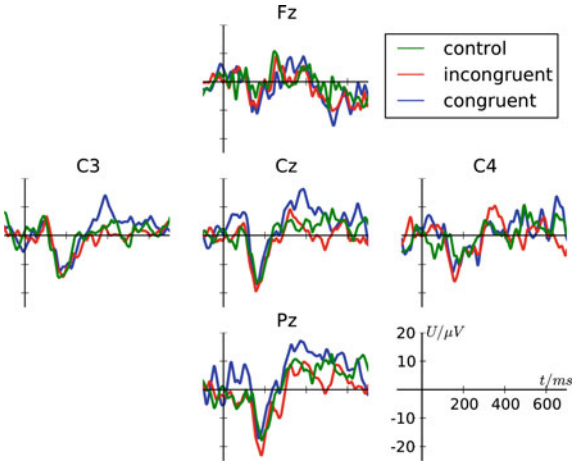

Fig. 79.5 Event-related potentials for electrodes Fz, C3, Cz, C4, and Pz. A prominent N200 can be observed, as well as more negative ERPs for the *incongruent* compared to the *congruent* condition between 300 and 500 ms poststimulus

79.3.3 Relationship Between EEG and BOLD

To quantify the correlation between event-related EEG power changes and BOLD responses, we performed the frequency- and distance-dependent analysis as described earlier. For statistical evaluation, we conducted a four-way repeated measure ANOVA with independent variables *radius* (seven levels), *frequency band* (six levels), *channel* (five levels), and *condition* (three levels) as within-subject factors and *correlation* as dependent variable. Data from 12 subjects were included (see above).

The results of this analysis are summarized in Table 79.1. We observed a main effect of *frequency band* ($F = 4.78$, $p < 0.001$) as well as an interaction between *radius* and *frequency band* ($F = 5.39$, $p < 0.001$). These effects indicate that the EEG–BOLD relationship depends on the frequency band and that it varies with the distance between EEG recording site and the fMRI voxels, yet not consistently across the frequency bands. For *radius*, we only observed a trend ($F = 1.71$, $p = 0.08$).

For the factor *channel* we neither observed a significant effect nor a significant interaction with one of the other factors. The same applies to the factor *condition.* Thus we disregarded these factors in our further analyses and only used the meta-condition "all," including all trials, and accumulated the data from all five channels.

To resolve the *radius* × *frequency band* interaction we performed one-way ANOVAs for each frequency band (Table 79.2). We attained significant effects for the δ, α, $\gamma_{1,}$ and γ_2 bands. The strongest effect was in the γ_1-band ($F = 7.62$, $p < 0.001$).

Table 79.1 Results for the four-way repeated measures ANOVA. Only significant interactions are listed, for all other interactions, $p > 0.05$

Factor/interaction	*F*	*p*
Radius	1.71	0.08
Frequency band	4.78	<0.001
Channel	0.72	0.58
Condition	0.83	0.46
Radius × frequency band	5.39	<0.001

Table 79.2 Results for one-way repeated measures ANOVAs using the factor *radius* for each frequency band

Frequency band	*F*	*p*
δ	5.76	<0.001
θ	1.89	0.08
α	5.79	<0.001
β	1.72	0.11
γ_1	7.62	<0.001
γ_2	5.35	<0.001

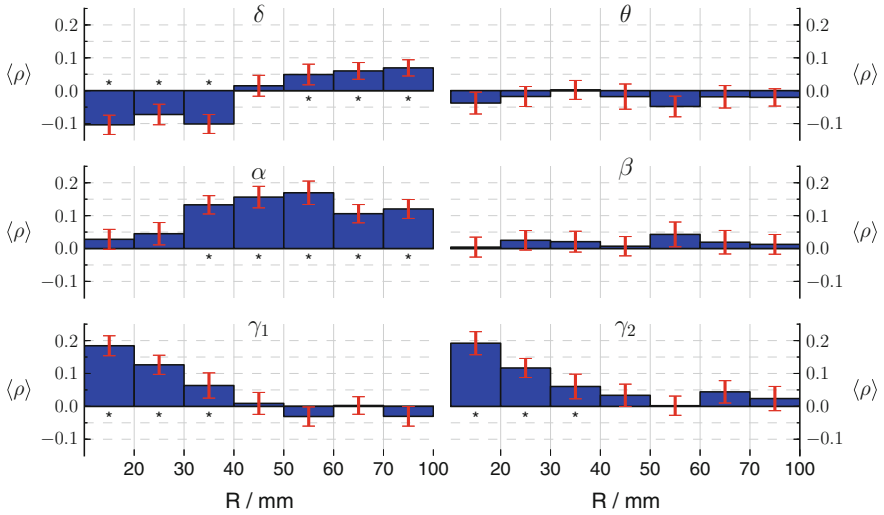

Fig. 79.6 Correlations between power in EEG bands $(\delta, \theta, \alpha, \beta, \gamma_1, \gamma_2)$ and average BOLD response within spherical shells with increasing radii $R^{\mathrm{I,O}}$ centered around the electrode locations. *Bars* denote the mean Spearman's rank correlation coefficients $\langle\rho\rangle$ across channels and subjects, *errorbars* the corresponding standard deviation. Correlation values were tested against zero using Student's t test, significant results are marked with *asterisk*. The statistical threshold was Bonferroni corrected for $N_{\mathrm{radii}} \times N_{\mathrm{bands}} = 42$, $p = \frac{0.05}{42} = 1.2 \times 10^{-3}$

To further disentangle the frequency band and radius dependence, we averaged the correlation coefficients across all channels and subjects. We applied a Fisher z transform to the values of ρ prior to averaging and the inverse transform afterward. These mean rank correlation coefficients are shown in Fig. 79.6. Average EEG–BOLD correlations in all cases were within the range $[-0.11, 0.21]$. We observed several radius/frequency band combinations for which EEG–BOLD correlations across subjects significantly differed from zero (even after applying Bonferroni correction), i.e., in these cases EEG–BOLD correlation appear to be stable across subjects and channels.

For the γ-bands we observed positive short-ranged (up to 40 mm) EEG–BOLD correlations which decreased for larger distances. For $R^{\mathrm{O}} > 40$ mm, no significant results were obtained.

In contrast to previous studies [7–9] investigating spontaneous EEG activity, our findings indicate positive EEG–BOLD correlations for the α-band. These correlations were not observed for small radii, and we only observed long-ranged correlations, beginning at a radius of $R^{\mathrm{I}} = 30$ mm.

For the θ- and β-bands we observed no significant EEG/BOLD correlations.

For the δ-band the EEG/BOLD correlations were negative for small distances and turned to positive values for larger distances.

79.4 Discussion

Using a cognitive paradigm addressing auditory conflict processing we have shown that the event-related EEG–BOLD relationship strongly varies for different frequency bands. These effects are moreover location specific because for four out of six frequency bands they clearly depend on the distance between fMRI voxel and the EEG recording site, i.e., they appear to be not related to large-scale or whole-brain fluctuations of neural activation.

The largest positive EEG–BOLD correlations were observed for the γ bands. These findings are in accordance with previous studies investigating ongoing EEG–BOLD correlations during presentations of film sequences [33] and LFP–BOLD correlations during visual chequerboard stimulation [33, 34]. A positive correlation between lower γ band activity (around 40 Hz) and BOLD effects has also been demonstrated during cognitive tasks, for instance, during working memory maintenance [18] and during an auditory choice experiment [35]. Furthermore, [36] found a positive EEG–BOLD correlation for the upper γ band (60–80 Hz) in a visual attention task known to elicit a pronounced increase of EEG activity in this frequency range.

For the δ range we observed a negative EEG–BOLD correlation for small distances between voxel and EEG recording site. This again is in accordance with previous studies investigating ongoing EEG–BOLD interrelations [33, 37, 38], as well as with the putative inhibitory function of the δ rhythm [21, 39]. For larger radii, the correlation inverts to positive values. This inversion possibly resembles spatial activation patterns related to lateral inhibition effects [40].

Several previous studies found negative correlations between ongoing EEG activity in the α-band and BOLD fluctuations [7–9]. Negative correlations between alpha power and fMRI activity were also observed in posterior regions during a visual attention task [36] and in sensorimotor areas during motor imagery and movements [41]. During visual working memory maintenance a negative correlation has been observed in occipital and middle temporal areas in one study [42]. In another study on visual working memory, a negative correlation between BOLD fluctuations and EEG in the upper α band (10–12 Hz) was detected for parietooccipital regions, but a positive correlation with EEG in the lower α band (8–10 Hz) was found for the medial prefrontal cortex, as well as for anterior and posterior cingulate cortexes [18]. Since the anterior cingulate cortex is well known to be involved in conflict processing [23, 30], the positive correlation with the α-band found at central electrode contacts in our study may be related to this previous observation. One may conclude that the correlation of event-related alpha power changes with BOLD responses strongly depends on brain region and cognitive task.

In summary, we observed pronounced influences of frequency and distance between EEG recording site and fMRI voxel on the correlation between event-related EEG perturbations and BOLD responses. The knowledge of these

frequency- and distance-dependent relations between EEG–activity and BOLD responses may serve as a basis for a common interpretation of combined EEG/fMRI studies.

Acknowledgments This work was financially supported by the BONFOR foundation (instrument 7).

References

1. Warach, S., Ives, J.R., Schlaug, G., Patel, M.R., Darby, D.G., Thangaraj, V., Edelman, R.R., Schomer, D.L.: EEG-triggered echo-planar functional MRI in epilepsy. Neurology **47**(1), 89–93 (1996)
2. Krakow, K., Woermann, F.G., Symms, M.R., Allen, P.J., Lemieux, L., Barker, G.J., Duncan, J.S., Fish, D.R.: EEG-triggered functional MRI of interictal epileptiform activity in patients with partial seizures. Brain **122**(9), 1679–1688 (1999)
3. Hoffmann, A., Jäger, L., Werhahn, K., Jaschke, M., Noachtar, S., Reiser, M.: Electroencephalography during functional echo-planar imaging: detection of epileptic spikes using post-processing methods. Magn. Reson. Med. **44**(5), 791–798 (2000)
4. Allen, P.: Identification of EEG events in the MR scanner: the problem of pulse artifact and a method for its subtraction. Neuroimage **8**(3), 229–239 (1998)
5. Allen, P.J., Josephs, O., Turner, R.: A method for removing imaging artifact from continuous EEG recorded during functional MRI. Neuroimage **12**(2), 230–239 (2000)
6. Niazy, R.K., Beckmann, C.F., Iannetti, G.D., Brady, J.M., Smith, S.M.: Removal of FMRI environment artifacts from EEG data using optimal basis sets. Neuroimage **28**(3), 720–737 (2005)
7. Goldman, R.I., Stern, J.M., Engel, J., Cohen, M.S.: Simultaneous EEG and fMRI of the alpha rhythm. NeuroReport **13**(18), 2487–2492 (2002)
8. Laufs, H., Kleinschmidt, A., Beyerle, A., Eger, E., Salek-Haddadi, A., Preibisch, C., Krakow, K.: EEG-correlated fMRI of human alpha activity. Neuroimage **19**(4), 1463–1476 (2003)
9. Moosmann, M., Ritter, P., Krastel, I., Brink, A., Thees, S., Blankenburg, F., Taskin, B., Obrig, H., Villringer, A.: Correlates of alpha rhythm in functional magnetic resonance imaging and near infrared spectroscopy. Neuroimage **20**(1), 145–158 (2003)
10. Bonmassar, G., Anami, K., Ives, J., Belliveau, J.W.: Visual evoked potential (VEP) measured by simultaneous 64-channel EEG and 3T fMRI. NeuroReport **10**(9), 1893–1897 (1999)
11. Kruggel, F., Wiggins, C., Herrmann, C., von Cramon, D.: Recording of the event-related potentials during functional MRI at 3.0 Tesla field strength. Magn. Reson. Med. **44**(2), 277–282 (2000)
12. Hanslmayr, S., Volberg, G., Wimber, M., Raabe, M., Greenlee, M.W., Bäuml, K.H.T.: The relationship between brain oscillations and BOLD signal during memory formation: a combined EEG-fMRI study. J.Neurosci. **31**(44), 15674–15680 (2011)
13. Czisch, M., Wetter, T., Kaufmann, C., Pollmächer, T., Holsboer, F., Auer, D.P.: Altered processing of acoustic stimuli during sleep: reduced auditory activation and visual deactivation detected by a combined fMRI/EEG study. Neuroimage **16**(1), 251–258 (2002)
14. Liebenthal, E., Ellingson, M.L., Spanaki, M.V., Prieto, T.E., Ropella, K.M., Binder, J.R.: Simultaneous ERP and fMRI of the auditory cortex in a passive oddball paradigm. Neuroimage **19**(4), 1395–1404 (2003)
15. Murta, T., Leite, M., Carmichael, D.W., Figueiredo, P., Lemieux, L.: Electrophysiological correlates of the BOLD signal for EEG-informed fMRI. Hum. Brain Mapp. (2014) n/a

16. Foucher, J., Otzenberger, H., Gounot, D.: The BOLD response and the gamma oscillations respond differently than evoked potentials: an interleaved EEG-fMRI study. BMC Neurosci. **4** (1), 22 (2003)
17. Salek-Haddadi, A., Friston, K.J., Lemieux, L., Fish, D.R.: Studying spontaneous EEG activity with fMRI. Brain Res. Brain Res. Rev. **43**(1), 110–133 (2003)
18. Michels, L., Bucher, K., Lüchinger, R., Klaver, P., Martin, E., Jeanmonod, D., Brandeis, D.: Simultaneous EEG-fMRI during a working memory task: modulations in low and high frequency bands. PLoS ONE **5**(4), e10298 (2010)
19. Laufs, H., Holt, J.L., Elfont, R., Krams, M., Paul, J.S., Krakow, K., Kleinschmidt, A.: Where the BOLD signal goes when alpha EEG leaves. Neuroimage **31**(4), 1408–1418 (2006)
20. Buzsáki, G., Draguhn, A.: Neuronal oscillations in cortical networks. Science **304**(5679), 1926–1929 (2004)
21. Birbaumer, N., Elbert, T., Canavan, A.G., Rockstroh, B.: Slow potentials of the cerebral cortex and behavior. Physiol. Rev. **70**(1), 1–41 (1990)
22. Stroop, J.R.: Studies of interference in serial verbal reactions. J. Exp. Psychol. **18**(6), 643–662 (1935)
23. Haupt, S., Axmacher, N., Cohen, M.X., Elger, C.E., Fell, J.: Activation of the caudal anterior cingulate cortex due to task-related interference in an auditory Stroop paradigm. Hum. Brain Mapp. **30**(9), 3043–3056 (2009)
24. Goldwave Inc.: Goldwave audio editing software. http://www.goldwave.com (2011)
25. Smith, S.M., Jenkinson, M., Woolrich, M.W., Beckmann, C.F., Behrens, T.E., Johansen-Berg, H., Bannister, P.R., De Luca, M., Drobnjak, I., Flitney, D.E., Niazy, R.K., Saunders, J., Vickers, J., Zhang, Y., De Stefano, N., Brady, J.M., Matthews, P.M.: Advances in functional and structural MR image analysis and implementation as FSL. Neuroimage **23**(Suppl 1), S208–S219 (2004)
26. Friston, K.J., Mechelli, A., Turner, R., Price, C.J.: Nonlinear responses in fMRI: the Balloon Model, Volterra Kernels, and other hemodynamics. Neuroimage **12**(4), 466–477 (2000)
27. Lorensen, W.E., Cline, H.E.: Marching cubes: a high resolution 3D surface construction algorithm. In: Proceedings of the 14th Annual Conference on Computer Graphics and Interactive Techniques, SIGGRAPH '87, vol. 21, pp. 163–169, New York, NY, USA, ACM (July 1987)
28. Smith, S.M.: Fast robust automated brain extraction. Hum. Brain Mapp. **17**(3), 143–155 (2002)
29. Carter, C.S., Van Veen, V.: Anterior cingulate cortex and conflict detection: an update of theory and data. Cogn. Affect. Behav. Neurosci. **7**(4), 367–379 (2007)
30. Hanslmayr, S., Pastotter, B., Bauml, K.H., Gruber, S., Wimber, M., Klimesch, W.: The electrophysiological dynamics of interference during the Stroop task. J. Cogn. Neurosci. **20**(2), 215–225 (2008)
31. Shor, R.E.: An auditory analog of the Stroop test. J. Gen. Psychol. **93**(2d Half), 281–288 (1975)
32. Coste, C.P., Sadaghiani, S., Friston, K.J., Kleinschmidt, A.: Ongoing brain activity fluctuations directly account for intertrial and indirectly for intersubject variability in Stroop task performance. Cereb. Cortex. **21**(11), 2612–2619 (2011)
33. Mukamel, R., Gelbard, H., Arieli, A., Hasson, U., Fried, I., Malach, R.: Coupling between neuronal firing, field potentials, and fMRI in human auditory cortex. Science **309**(5736), 951–954 (2005)
34. Logothetis, N.K., Pauls, J., Augath, M., Trinath, T., Oeltermann, A.: Neurophysiological investigation of the basis of the fMRI signal. Nature **412**(6843), 150–157 (2001)
35. Mulert, C., Leicht, G., Hepp, P., Kirsch, V., Karch, S., Pogarell, O., Reiser, M., Hegerl, U., Jäger, L., Moller, H.J.: Single-trial coupling of the gamma-band response and the corresponding BOLD signal. Neuroimage **49**(3), 2238–2247 (2010)

36. Scheeringa, R., Fries, P., Petersson, K.M.M., Oostenveld, R., Grothe, I., Norris, D.G., Hagoort, P., Bastiaansen, M.C.: Neuronal dynamics underlying high- and low-frequency EEG oscillations contribute independently to the human BOLD signal. Neuron **69**(3), 572–583 (2011)
37. Czisch, M., Wehrle, R., Kaufmann, C., Wetter, T.C., Holsboer, F., Pollmächer, T., Auer, D.P.: Functional MRI during sleep: BOLD signal decreases and their electrophysiological correlates. Eur. J. Neurosci. **20**(2), 566–574 (2004)
38. Makiranta, M.: BOLD-contrast functional MRI signal changes related to intermittent rhythmic delta activity in EEG during voluntary hyperventilation? Simultaneous EEG and fMRI study. Neuroimage **22**(1), 222–231 (2004)
39. Fernández, T., Harmony, T., Silva-Pereyra, J., Fernández-Bouzas, A., Gersenowies, J., Galán, L., Carbonell, F., Marosi, E., Otero, G., Valdés, S.I.: Specific EEG frequencies at specific brain areas and performance. Neuroreport **11**(12), 2663–2668 (2000)
40. Severens, M., Farquhar, J., Desain, P., Duysens, J., Gielen, C.: Transient and steady-state responses to mechanical stimulation of different fingers reveal interactions based on lateral inhibition. Clin. Neurophysiol. **121**(12), 2090–2096 (2010)
41. Yuan, H., Liu, T., Szarkowski, R., Rios, C., Ashe, J., He, B.: Negative covariation between task-related responses in alpha/beta-band activity and BOLD in human sensorimotor cortex: An EEG and fMRI study of motor imagery and movements. Neuroimage **49**(3), 2596–2606 (2010)
42. Scheeringa, R., Petersson, K.M., Oostenveld, R., Norris, D.G., Hagoort, P., Bastiaansen, M.C. M.: Trial-by-trial coupling between EEG and BOLD identifies networks related to alpha and theta EEG power increases during working memory maintenance. Neuroimage **44**(3), 1224–1238 (2009)